ELSEVIER

Journal of Magnetism and Magnetic Materials 183 (1998) 348–355

journal of magnetism and magnetic materials

Critical behaviour near the ferromagnetic–paramagnetic phase transition in $La_{0.8}Sr_{0.2}MnO_3$

Ch.V. Mohan[a,b,*], M. Seeger[a], H. Kronmüller[a], P. Murugaraj[c], J. Maier[c]

[a] *Max-Planck Institut für Metallforschung, Heisenbergstr. 1, D-70569 Stuttgart, Germany*
[b] *Max-Planck Institut für Mikrostrukturphysik, Weinberg 2, D-06120 Halle (Saale), Allemagne, Germany*
[c] *Max-Planck Institut für Festkörperforschung, Heisenbergstr. 1, D-70569 Stuttgart, Germany*

Received 4 September 1997

Abstract

We have investigated the critical behaviour of a $La_{0.8}Sr_{0.2}MnO_3$ polycrystalline sample near its ferromagnetic – paramagnetic phase transition temperature by determining the critical exponents corresponding to various thermodynamical quantities. Such a study is very important and interesting because this magnetic phase transition is associated with a simultaneous electronic phase transition, i.e. a metal–insulator transition. In this paper, we report our results on this magnetic phase transition analysed through various techniques like the modified Arrott plots, Kouvel–Fisher method, scaling-equation-of-state analysis and the critical magnetisation isotherm. The values deduced for the critical exponents are in good agreement with those predicted, theoretically, for the mean field theory, indicating that the exchange interaction is of long-range type.

PACS: 75.40.Cx; 75.30.Kz; 75.50.Dd

Keywords: Phase transition – magnetic; Phase transition – electronic; Critical exponents; Long-range interactions

1. Introduction

The hole-doped $LaMnO_3$ perovskites are drawing a lot of interest of the scientific community [1–3] due to their highly interesting and unresolved properties. The antiferromagnetic insulator $LaMnO_3$ becomes a ferromagnetic metal upon doping with Sr [4–7]. Therefore, the $La_{1-x}Sr_xMnO_3$ system provides an opportunity to study a number of important physical problems. Mixed valence state for Mn (Mn^{3+}/Mn^{4+}) has been observed in these systems with three types of, i.e. structural, magnetic and electronic transitions. Due to the large transfer energy from holes hopping in the e_g band, the ferromagnetic exchange between the nearest neighbour Mn spins is predicted to be very strong [8]. It was already reported that an applied field can drive

* Corresponding author. Tel.: + 49 345 5582630; fax: + 49 345 5511223; e-mail: mohan@mpi-halle.mpg.de.

0304-8853/98/$19.00
PII S0304-8853(97)01095-0

a structural phase transition in $La_{0.825}Sr_{0.175}MnO_3$ [9]. The volume contraction appearing at the metal–insulator transition has a relatively small contribution from the changes in magnetism, i.e. ferromagnetic to paramagnetic behaviour. It is important to study these two transitions individually and thoroughly which will give an idea about the nature and type of interaction between these two transitions. In other words, studying the electronic and magnetic phase transition separately will give us information about the effect of one on the other. In the literature, there are published some controversial results concerning the critical exponent β. Morrish [10] has found a rather high value $\beta = 0.495$ in a $La_{0.65}Pb_{0.44}MnO_3$ crystal, which is in good agreement with recent results from Lofland et al. [11] found in the composition $La_{0.7}Sr_{0.3}MnO_3$ ($\beta = 0.45$), indicating a mean-field-like behaviour at magnetic phase transition. In contrast to this, neutron scattering experiments yielded a rather low β value (0.295) [12]. However, to fully describe the behaviour at phase transition, not only the ferromagnetic range but also the paramagnetic range has to be studied so that the complete set of critical exponents β, γ and δ can be determined. Therefore, our group which is working on magnetic phase transitions in various classes of materials has undertaken a detailed study on the determination of critical exponents for these systems. We have chosen the composition $La_{0.8}Sr_{0.2}MnO_3$ which has a Curie temperature very close to the room temperature since this composition shows a magnetic phase transition associated with a simultaneous electronic phase transition.

2. Experimental details

Lanthanum strontium manganese oxide with formula $La_{0.8}Sr_{0.2}MnO_3$ was prepared by the conventional ceramic route. The starting materials used in the preparation of the compound were all high-purity grade from Alfa products. Appropriate proportions of lanthanum oxide, strontium carbonate and manganese dioxide are weighed to arrive at the stoichiometry $La_{0.8}Sr_{0.2}MnO_x$. The weighed components are then wet mixed and milled using a Retsch vibromill fitted with bowl and ball made of tungsten carbide material. This mixture is then calcined at 1100°C for 20 h with three intermediate grindings/mixing to ensure homogeneous mixing and reaction. X-ray diffraction analysis have been performed on the powder sample using Philips X-ray powder diffractometer (model PW 3710) in the 2θ range 10–100°. The diffraction data on this powder (shown in Fig. 1) showed the formation of phase-pure $La_{0.8}Sr_{0.2}MnO_x$ compound. The impurity phases if present are below the detection limit of X-ray diffraction analysis (less than 1%). All the observed diffraction peaks could be fitted to the d-spacings of the reported [13] pattern of lanthanum strontium manganate. Wet chemical analysis was performed on this sample powder by inductively coupled plasma (ICP) technique. The analytical results confirmed the stoichiometry of the powder to the formula indicated. The resulting powder was then binded with 1 wt% solution of polyvinyl alcohol (PVA) in water, granulated and uniaxially pressed into discs using conventional dies. These discs are then sintered at 1500°C for 5 h. Enough care is taken to burn off the binder material before the sintering stage so that there are

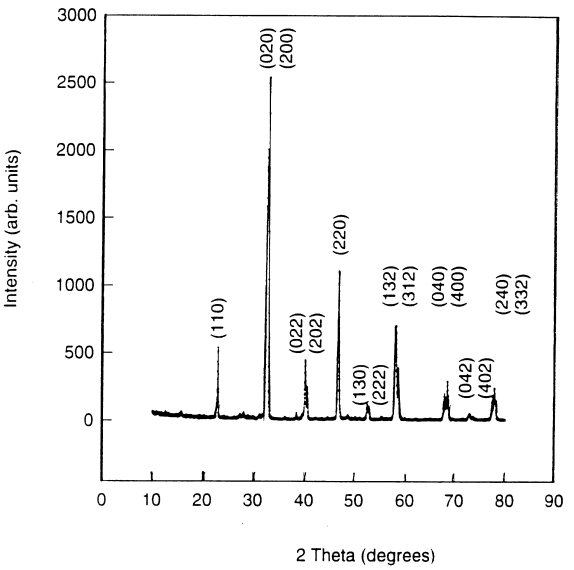

Fig. 1. X-ray diffractogram recorded on $La_{0.8}Sr_{0.2}MnO_3$ polycrystalline sample. All the peaks observed have been indexed.

no entrapped gases in the sample. These samples are annealed at 1300°C for 10 h in ambient atmosphere to ensure homogeneous distribution of the substituted cations. The X-ray diffraction analysis of these samples yielded the lattice constants as follows (in angstrom units): $a_0 = 5.4634 \pm 0.0082$; $b_0 = 5.5272 \pm 0.0026$; $c_0 = 7.7514 \pm 0.0230$ and $\beta = 90.86 \pm 0.16^\circ$. The density of the sintered material was measured using micromeritics pycnometer (Model Accu Pyco 1330) which was found to be 6.2358 g/cm^3 (approximately 98% of the theoretical density). The sample showed a ferromagnetic to paramagnetic phase transition at about 315 K.

The magnetisation measurements have been performed using a SQUID magnetometer (Model: MPMS). In order to have an estimation of the Curie temperature before we start our measurements in the critical region, we have performed kink-point measurements in the presence of an applied, but small, field. These measurements show a very good transition from ferromagnetic to paramagnetic state approximately at 315 K. The magnetisation isotherms are then recorded in the temperature range $270\,\mathrm{K} \leqslant T \leqslant 348\,\mathrm{K}$ which embraces the critical region. These isotherms are recorded at temperature intervals of 0.25 K close to T_C (0.5 and 1 K for temperatures away from T_C) and the temperature values are stabilised to within ± 10 mK. The demagnetisation factor is obtained from the slope of the low-field data and the demagnetisation corrections are made in order to obtain the internal field values. Typical magnetisation isotherms are shown in Fig. 2 for a few representative temperatures. Note that the field values used in this figure are the field values obtained after correcting for demagnetisation.

3. Results and data analysis

3.1. Methods of analysis

We would like to make a brief mention of the definitions of various critical exponents that could be obtained from the magnetisation data. The second-order magnetic phase transition occurring at the Curie point is characterised by a set of critical

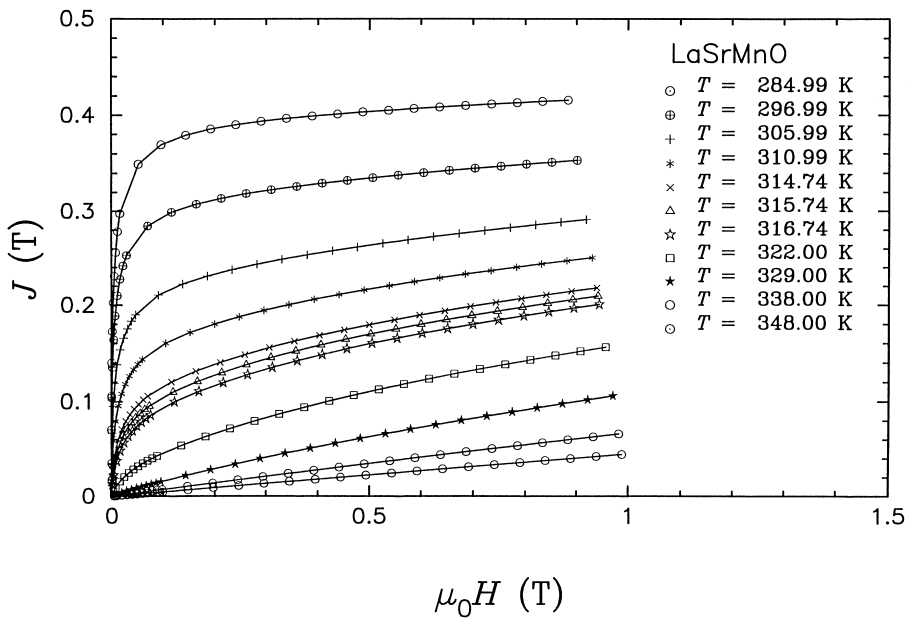

Fig. 2. Magnetisation data recorded on $La_{0.8}Sr_{0.2}MnO_3$ sample at a few representative temperatures.

exponents, β (corresponding to the spontaneous magnetisation), γ', γ (corresponding to the initial susceptibility) and δ (corresponding to the critical magnetisation isotherm), which are defined as

$$J_s(T) = J_0(-\varepsilon)^{\beta}, \quad \varepsilon < 0, \tag{1}$$

$$\chi'^{-1}_0(T) = (h_0/J_0)\varepsilon^{\gamma'}, \quad \varepsilon < 0, \tag{2}$$

$$\chi_0^{-1}(T) = (h_0/J_0)\varepsilon^{\gamma}, \quad \varepsilon > 0, \tag{3}$$

$$J = A_0(\mu_0 H)^{1/\delta}, \quad \varepsilon = 0, \tag{4}$$

where ε stands for the reduced temperature defined as $\varepsilon = (T - T_C)/T_C$, T_C is the Curie temperature and J_0, h_0/J_0 and A_0 denote the critical amplitudes.

To determine the exponents β and γ, we first apply the modified Arrott plots [14,15] method based on the Arrott–Noakes equation of state [16] given by

$$(\mu_0 H/J)^{1/\gamma} = (T - T_C)/T_1 + (J/J_1)^{1/\beta}, \tag{5}$$

where T_1 and J_1 are some constants which are characteristic of the material under investigation.

According to this method, the original magnetisation data are converted into the modified Arrott, i.e. $J^{1/\beta}$ versus $(\mu_0 H/J)^{1/\gamma}$, plots through the choice of critical exponents β and γ that makes the $J^{1/\beta}$ versus $(\mu_0 H/J)^{1/\gamma}$ isotherms in a narrow temperature range around T_C straight and parallel to one another over as wide a range of $(\mu_0 H/J)$ values as possible.

Linear extrapolation of the high-field straight line portions of the isotherms to $(\mu_0 H/J)^{1/\gamma} = 0$ and $J^{1/\beta} = 0$ yields intercepts on the $J^{1/\beta}$ and $(\mu_0 H/J)^{1/\gamma}$ axes from which the spontaneous magnetisation $J_s(T)$ and the inverse initial susceptibility $\chi_0^{-1}(T)$ are computed. From these data, the parameters T_C, β and γ are obtained by using the Kouvel–Fisher [17] method, which can be explained as follows.

The Kouvel–Fisher (KF) method is based on the equations

$$J_s(T)[\mathrm{d}J_s(T)/\mathrm{d}T]^{-1} = (T - T_C)/\beta \tag{6}$$

and

$$\chi_0^{-1}(T)[\mathrm{d}\chi_0^{-1}(T)/\mathrm{d}T]^{-1} = (T - T_C)/\gamma, \tag{7}$$

which hold good in the critical region.

According to these equations, the quantities $J_s(T)[\mathrm{d}J_s(T)/\mathrm{d}T]^{-1}$ and $\chi_0^{-1}(T)[\mathrm{d}\chi_0^{-1}(T)/\mathrm{d}T]^{-1}$ plotted against temperature, yield straight lines with slopes $(1/\beta)$ and $(1/\gamma)$, respectively, and the intercepts on the T-axes are equal to T_C.

Another independent way to determine the exponents β, γ' and γ is by using scaling theory [18] which predicts the existence of a reduced equation of state of the form

$$J/|\varepsilon|^{\beta} = f_{\pm}(\mu_0 H/|\varepsilon|^{\beta+\gamma}), \tag{8}$$

where $(+)$ and $(-)$ signs represent data for temperatures above (paramagnetic) and below (ferromagnetic) the Curie temperature, respectively. This relation further implies that $J/|\varepsilon|^{\beta}$ as a function of $\mu_0 H/|\varepsilon|^{\beta+\gamma}$ falls on two different curves, one for temperatures below T_C and the other for temperatures above T_C.

The exponent δ can be obtained from the slope of the ln J versus ln $(\mu_0 H)$ plot at T_C.

3.2. Analysis of the data

The isothermal magnetisation data (Fig. 2) have been converted into the form of the modified Arrott plots and these plots are shown in Fig. 3. The linearity of these isotherms in the high-field region and the finding that these isotherms are almost parallel to one another guarantee that the exponents β and γ determined in this way are very much accurate (at least to within 5%). The values of these exponents are given in the figure. This particular choice of the exponents is achieved by varying these values over a large range and by checking the modified Arrott plots for each and every choice of the exponent values. The temperature variation of the spontaneous magnetisation ($J_s(T)$) and the inverse initial susceptibility ($\chi_0^{-1}(T)$), obtained as explained in the earlier part of this section, is depicted in Figs. 4 and 5, respectively. These data are indicated by the open symbols in these plots. The continuous curves in Figs. 4 and 5 belong to the power-law fit obtained with the help of Eqs. (1) and (3), respectively. From these data, the quantities $J_s(T)[\mathrm{d}J_s(T)/\mathrm{d}T]^{-1}$ and $\chi_0^{-1}(T)[\mathrm{d}\chi_0^{-1}(T)/\mathrm{d}T]^{-1}$ are computed. The $J_s(T)[\mathrm{d}J_s(T)/\mathrm{d}T]^{-1}$ versus

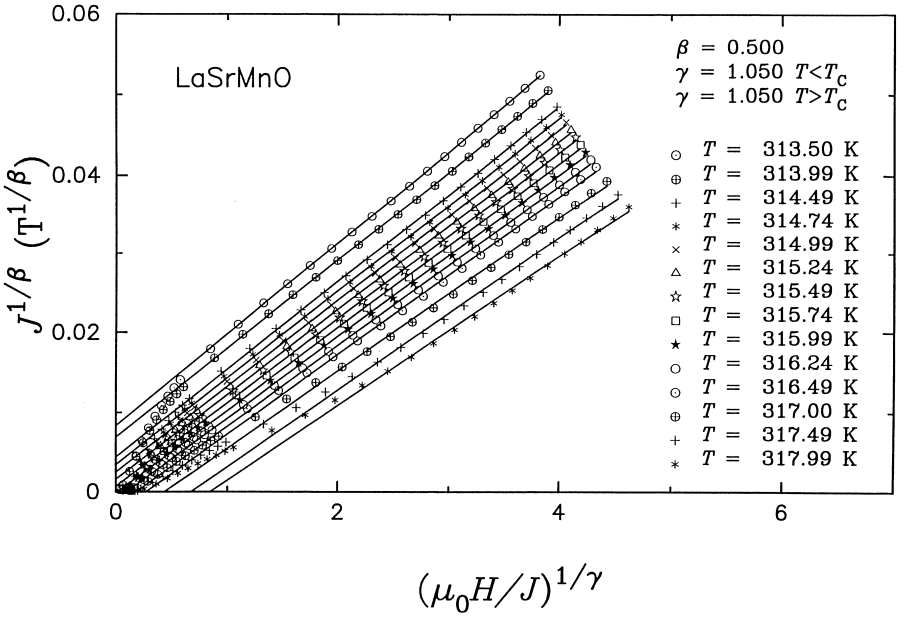

Fig. 3. Modified Arrott plot isotherms on $La_{0.8}Sr_{0.2}MnO_3$. The values of exponents used have also been shown in the figure.

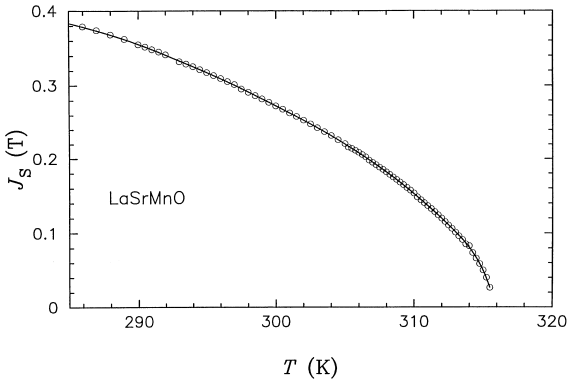

Fig. 4. The temperature variation of the spontaneous magnetisation along with the fit obtained with the help of the power law.

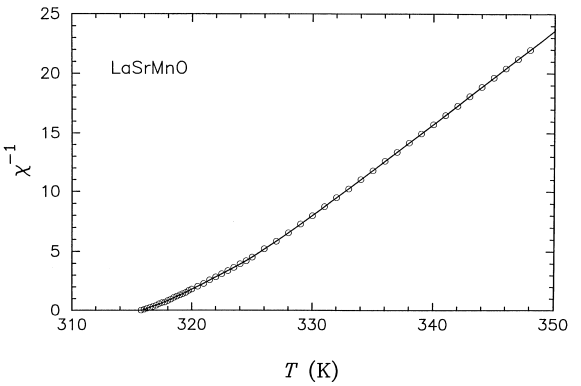

Fig. 5. The temperature variation of the inverse initial susceptibility along with the fit obtained with the help of the power law.

T and $\chi_0^{-1}(T)[\mathrm{d}\chi_0^{-1}(T)/\mathrm{d}T]^{-1}$ versus T plots are shown in Figs. 6 and 7, respectively. The straight line in these figures represents the least-squares fit to the data based on Eqs. (6) and (7). The ln J versus $\ln(\mu_0 H)$ plots are also constructed and these plots are shown in Fig. 8. The straight line in this figure represents the fit obtained for the data at T_C based on Eq. (4).

Now, the values of the critical exponents obtained are $\beta = 0.50 \pm 0.02$, $\gamma' = 1.05 \pm 0.03$, $\gamma = 1.08 \pm 0.03$ and $\delta = 3.13 \pm 0.20$. The value of exponent δ calculated from the Widom scaling relation

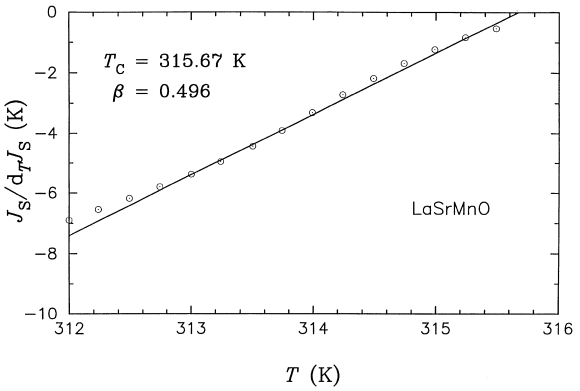

Fig. 6. Kouvel–Fisher plot for the spontaneous magnetisation.

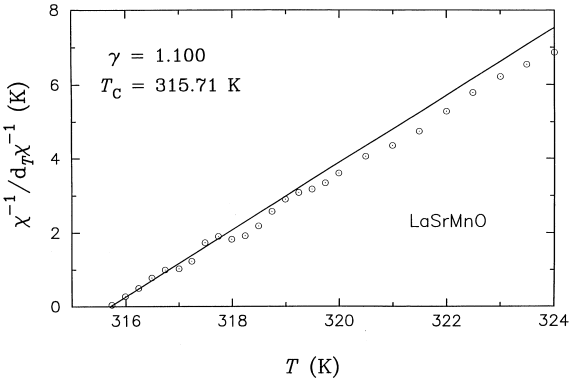

Fig. 7. Kouvel–Fisher plot for the inverse initial susceptibility.

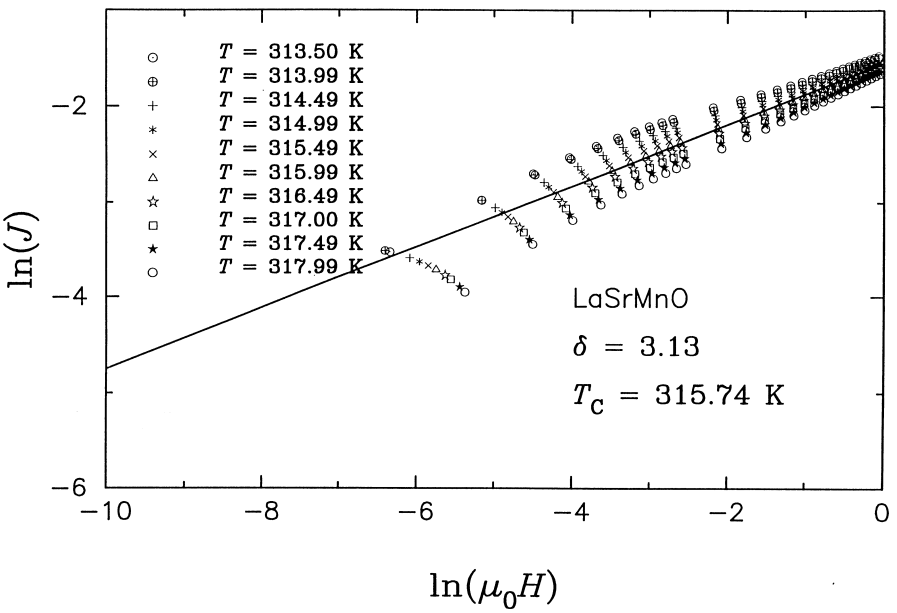

Fig. 8. ln J versus ln($\mu_0 H$) plots for $La_{0.8}Sr_{0.2}MnO_3$.

($\delta = 1 + \gamma'/\beta = 1 + \gamma/\beta$) with the help of the exponent values mentioned above is in a very close agreement with the value of δ given above which is obtained from the critical magnetisation isotherm. Validity of the Widom scaling relation demands that the magnetisation data should obey the scaling equation of state. The scaling plot obtained is shown in Fig. 9. A very good collapse of the magnetisation data in a small temperature range around T_C (the critical region) at various field values onto two different curves, one for temperatures below and the other for temperatures above the Curie temperature, indicates that the values of T_C and the exponents are accurate enough.

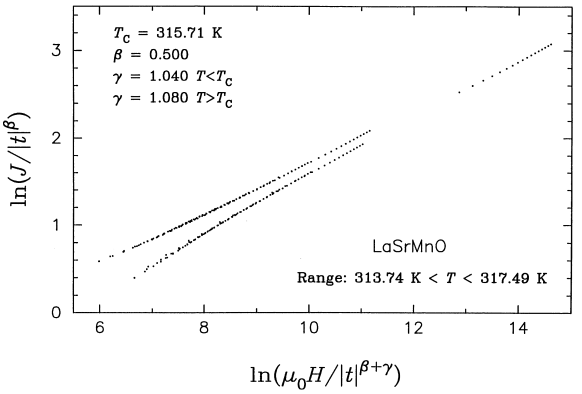

Fig. 9. The scaling plots for $La_{0.8}Sr_{0.2}MnO_3$.

4. Discussion

The experimentally determined values of the critical exponents, which are mentioned above, are compared with those predicted, theoretically, for the three-dimensional short-range isotropic Heisenberg model (the theoretical values for β, γ and δ are equal to 0.365, 1.386 and 4.800, respectively) and for the mean field theory ($\beta = 0.50$, $\gamma = 1.0$ and $\delta = 3.0$) which holds if the exchange interaction is of long-range type. In the case of exponent β, this result agrees with Refs. [10,11]. Fisher et al. [19] have done a renormalisation group analysis for the critical exponents of systems with long-range exchange interactions of the form $J(r) \propto 1/r^{d+\sigma}$ where d is the dimension of the system and σ is a measure of the range of the interaction. For $\sigma > 2$ (short-range interactions) the exponents are the ones of the nearest-neighbour model. For $\sigma > \frac{1}{2}$ (long-range order), the mean field exponents describe the critical behaviour. In the case of $\frac{1}{2} < \sigma < 2$, (mid-range order) the exponents depend on the parameter σ. A good agreement has been observed between our experimental values and the theoretical values of the mean field theory, indicating that the exchange interactions in this class of materials are of long-range type. It should be noted that the analysis of the critical exponents was performed in a rather small temperature range, i.e. $\varepsilon \leqslant 0.8\%$ in the case of Kouvel–Fisher plots and $\varepsilon \leqslant 0.6\%$ in the case of scaling analysis. The modified Arrott plot can be optimised to only one isotherm closest to T_C in the whole temperature range. In other words, the isotherm measured at $T = 315.74$ K is closer than $\varepsilon = 0.02\%$ at T_C and fulfils the equation of state (Eq. (5)) with the given exponent values. Therefore, we assume that our analysis of the critical exponents was carried out within the critical temperature range.

The observation of a low value for β by Martin et al. [12] may be attributed to the fact that most of the data used, in order to deduce the critical exponents, fall very much outside the critical region. However, the magnetic phase transition in this [12] sample ($La_{0.7}Sr_{0.3}MnO_3$) represents a phase transition from ferromagnetic metal to paramagnetic metal state.

5. Conclusions

In order to deduce the critical behaviour of the $La_{0.8}Sr_{0.2}MnO_3$ polycrystalline sample, we have performed accurate bulk magnetisation measurements using SQUID magnetometer near its ferromagnetic–paramagnetic phase transition temperature. The critical exponents are derived using the conventional ways of analysing the phase transitions. We found that these values are in a close agreement with those predicted for the mean field theory. The reason for this behaviour may be long-range interactions.

Acknowledgements

Two of the authors (ChVM and PM) thank the Max-Planck Society for financial assistance.

References

[1] G.H. Jonker, J.H. van Santen, Physica 16 (1950) 337.
[2] E.O. Wollan, W.C. Köhler, Phys. Rev. 100 (1955) 545.
[3] G.H. Jonker, Physica 22 (1956) 707.
[4] C. Zener, Phys. Rev. 82 (1951) 403.
[5] P.W. Anderson, H. Hasegawa, Phys. Rev. 100 (1955) 675.
[6] P.G. de Gennes, Phys. Rev. 100 (1955) 564.
[7] K. Kubo, N. Ohata, J. Phys. Soc. Japan 33 (1972) 21.
[8] N. Furukawa, J. Phys. Soc. Japan 63 (1994) 3214.

[9] A. Asamitsu, Y. Moritomo, Y. Tomioka, T. Arima, Y. Tokura, Nature (London) 373 (1995) 407.
[10] A.H. Morrish, in: Y. Hoshina, S. Tida, M. Sugimota (Eds.), International Conference on Ferrites, University Park Press, Baltimore, 1970, p. 574.
[11] S.E. Lofland, V. Ray, P.H. Kim, S.M. Bhagat, M.A. Manheimer, S.D. Tyagi, Phys. Rev. B 55 (1997) 2749.
[12] M.C. Martin, G. Shirane, Y. Endoh, K. Hirota, Y. Moritomo, Y. Tokura, Phys. Rev. B 53 (1996) 14285.
[13] JCPDS file 40-1000.
[14] Ch.V. Mohan, H. Kronmüller, J. Magn. Magn. Mater. 163 (1996) 96 and references cited therein.
[15] A.A. Coelho, Ch.V. Mohan, S. Gama, H. Kronmüller, J. Magn. Magn. Mater. 163 (1996) 87.
[16] A. Arrott, J.E. Noakes, Phys. Rev. Lett. 19 (1967) 786.
[17] J.S. Kouvel, M.E. Fisher, Phys. Rev. A 136 (1964) 1626.
[18] S.N. Kaul, J. Magn. Magn. Mater. 53 (1985) 5.
[19] M.E. Fisher, S.K. Ma, B.G. Nickel, Phys. Rev. Lett. 29 (1972) 917.